Hindawi
Wireless Communications and Mobile Computing
Volume 2021, Article ID 5536726, 8 pages
https://doi.org/10.1155/2021/5536726

Research Article

Intelligent Spectrum Management and Trajectory Design for UAV-Assisted Cognitive Ambient Backscatter Networks

Jiazhou Liu,[1] Sa Xiao,[2,3] Huayan Guo,[4] Xiangwei Zhou,[5] and Shixin He[1]

[1]*China Academy of Electronics and Information Technology, Beijing, China*
[2]*National Key Laboratory of Science and Technology on Communications, University of Electronic Science and Technology of China, 611731, China*
[3]*Institute of Electronic and Information Engineering of UESTC in Guangdong, 523808, China*
[4]*Shenzhen Research Institute, Hong Kong University of Science and Technology, Shenzhen, China*
[5]*Division of Electrical and Computer Engineering, Louisiana State University, Baton Rouge, LA, USA*

Correspondence should be addressed to Sa Xiao; xiaosa@uestc.edu.cn

Received 22 February 2021; Revised 3 March 2021; Accepted 11 March 2021; Published 7 April 2021

Academic Editor: Xin Liu

In this paper, we consider a novel *Internet of Things* (IoT) system in smart city called *unmanned aerial vehicle-* (UAV-) assisted cognitive backscatter network, where a UAV is employed as both a relay and a radio frequency source to help the data transmission between ground IoT *backscatter devices* (BDs) and a remote *data center* (DC). However, since the IoT applications are usually not assigned dedicated spectrum resource in smart cities, these data transmissions from BDs to the DC should share the licensed spectrum of *cellular users* (CUs). Therefore, we aim to maximize the minimum uplink throughput among all BDs while avoiding severe interference to CUs via joint spectrum management and UAV trajectory design. To solve the problem, we propose an iterative method utilizing block coordinated decent to partition the variables into two blocks. For the spectrum management problem, we first prove its convexity with the transmit power and time scheduling and then propose a two-step method to solve the two variables sequentially. For the UAV trajectory design problem, we resort to the fractional programming method to handle it. Simulation results demonstrate that the proposed algorithm can significantly increase the average max-min rate of the BDs while guaranteeing the acceptable interference to CUs with a fast convergence speed.

1. Introduction

The *Internet of Things* (IoT) is one of the most important application scenarios for the *fifth-generation* (5G) wireless communications. It enables different smart devices to connect with each other via wireless networks, thus has a great potential to remould vertical industries such as manufacturing, agriculture, urban-construction, and transportation [1, 2]. Since the IoT allows massive devices to access wireless networks, however, it also faces various practical challenges in its deployment [3]. For one thing, the IoT devices are usually too small to equip with high-capacity batteries. For another, massive deployed IoT devices may also exacerbate spectrum scarcity problems [4]. As a result, future widespread IoT applications highly require energy- and spectrum-efficient wireless communications techniques [5, 6].

In recent years, *ambient backscatter communications* (AmBC) has emerged as a cutting-edge technique in IoT networks [7–9]. With it, IoT devices are able to transmit by intentionally changing their own antenna impedances to reflect surrounding ambient *radio frequency* (RF) signals, e.g., TV or WiFi signals, instead of self-generated RF signals. Therefore, it neither requires any power-hungry circuit components such as the oscillators and analog-to-digital converters, nor additional spectrum resource for data transmission in AmBC [10]. As a result, AmBC has been considered as a promising candidate to support future IoT applications with stringent spectrum and energy constraints [11]. Due to the double fading effect with backscatter links

and direct interference from ambient RF signals, however, AmBC is usually reliable at distances of tens of meters. Moreover, the transmission length becomes much shorter if the *backscatter devices* (BDs) are buried under other objects. Therefore, increasing the coverage range as well as improving the link quality is the critical issues for the application of AmBC in large-scale IoT scenarios, e.g., smart agriculture or smart city [12, 13].

Mounted with miniaturized communication transceivers, *unmanned aerial vehicles* (UAVs) can work as mobile relays to provide reliable wireless connectivity between distant ground devices. Compared with traditional terrestrial relays, UAV relays are in general more flexible and cost-effective to deploy and likely to have better communication links due to the high chance of *line-of-sight* (LoS) links [14, 15]. Therefore, exploiting the agility of UAVs to build dual-hop LoS communication links is an efficient way to enhance the coverage of AmBC.

There has been some preliminary work regarding UAV-assisted relaying communications. In [16], an energy-efficient cooperative relaying scheme has been proposed for a UAV-assisted relaying network, while in [17], joint power allocation and trajectory design have been investigated to maximize the end-to-end throughput of UAV-assisted relaying transmission. Note that both studies focus on UAV communications in traditional cellular systems. In backscatter-enabled systems, the UAV needs to work as a RF source for the BDs in addition to being a relay. Therefore, novel trajectory design and resource scheduling schemes are required to deal with the coexistence of cellular and backscatter communications. Although the hardware prototype of UAV-assisted backscatter communications has been realized in [18], it still lacks theoretical analysis and optimization for the whole system.

In this paper, we consider a UAV-assisted cognitive backscatter network, where a UAV is not only employed as a relay to provide wireless connectivity between a remote *data center* (DC) and BDs but also works as the RF source for these BDs. However, since the IoT applications are usually not assigned dedicated spectrum resource in smart cities, the data transmission from BDs to the DC should share the spectrum licensed to *cellular users* (CUs). Therefore, we aim to maximize the minimum uplink rate among all BDs while avoiding severe interference to adjacent CUs via joint trajectory design and spectrum management. To achieve this objective, we propose an iterative method utilizing *block coordinated decent* (BCD) [19] to partition the variables into the time scheduling and power control variable and the trajectory design variable. For the former one, a two-step method is proposed to solve the transmit power and time scheduling sequentially, while for the latter one, we resort to the *fractional programming* (FP) method [20]. Both the convergence and complexity of the proposed algorithm are demonstrated by simulation results.

The rest of the paper is organized as follows. In Section 2, we describe the system model and formulate the optimization problem. To solve the problem, we develop a BCD and FP based iterative method in Section 3. Then, we present simulation results in Section 4. Finally, conclusions are drawn in Section 5.

2. System Model and Problem Formulation

2.1. System Model. We consider a UAV-assisted cognitive backscatter network as shown in Figure 1, where M BDs are fixed within an area without terrestrial networks and a UAV is employed as a relay for the data transmission from the BDs to a remote DC. The BDs are able to access the UAV via reflecting the relaying signals transmitted from it in a cyclical *time-division multiple access* (TDMA). The UAV works in *full-duplex* (FD) mode and can adjust its trajectory to improve the connectivity quality. Since the IoT applications are usually not assigned dedicated spectrum resource, the data transmission from the BDs to the DC cannot severely interfere the data reception at the adjacent CU. For analysis simplicity, we assume that the whole period is equally divided into K time slots, where K is sufficiently large so that the UAV is approximately stationary within each time slot. In addition, the location information of the UAV, BDs, and the CU is assumed to be available at the DC. The frame structure is shown in Figure 2. Specially, $\beta_{m,k}$ is denoted as the portion of time assigned to BD m in time slot k.

In this paper, we adopt 3D Cartesian coordinate as in [21]. Specially, the DC is set as the origin. The horizontal coordinates of BD m and the CU are fixed as $l_m = [x_m, y_m]^{\mathrm{T}}$ and $l_0 = [x_0, y_0]^{\mathrm{T}}$, respectively, and the corresponding altitudes are denoted as H_m and H_0, respectively. The UAV flies at a fixed altitude H, and its horizontal coordinate at time slot k is denoted as $q_k = [x_u[k], y_u[k]]^{\mathrm{T}}$. The cellular links from the UAV to the DC, and the CU and the dyadic backscatter link between BD m and the UAV all follow the free-space path loss model. Then, the corresponding channel power gain is given by

$$g[k] = \frac{\gamma_2}{H^2 + \|q_k\|^2},$$

$$g_0[k] = \frac{\gamma_2}{(H - H_0)^2 + \|q_k - l_0\|^2},$$

$$h_m[k] = \frac{\gamma_1}{\left[(H - H_m)^2 + \|q_k - l_m\|^2\right]^2}, \tag{1}$$

respectively, where γ_2 and γ_1 are the corresponding channel powers at distance of 1 m. Additionally, the channel power gain of the *self-interference* (SI) channel is denoted as ζ, whose value is determined by the adopted SI cancellation scheme.

Let $s_m[k\,; n]$ denote the signal transmitted from BD m during the n-th symbol period in time slot k. Assume the *decoded-and-forward* (DF) mode is adopted by the UAV. Then, the corresponding relay signal transmitted by the UAV is $s_m[k\,; n - \tau]$, where τ is the processing delay. As mentioned before, since the BDs do not have any active circuit to generate RF signals, they need to reflect the received relay signals for data transmission (for the initial τ symbol reception, the UAV can transmit any RF waveforms to the BDs). As a result, the received signals at the UAV and DC can be expressed as

$$y_m^{(1)}(k;n) = \sqrt{h_m[k]P_k}\alpha s_m(k;n-\tau)s_m(k;n) + \underbrace{\sqrt{\zeta P_k}s_m(k;n-\tau)}_{\text{SI}} + z_1(k;n),$$

$$y_m^{(2)}(k;n) = \sqrt{g[k]P_k}s_m(k;n-\tau) + z_2(k;n), \quad (2)$$

respectively, where P_k denotes the transmit power of the UAV at slot k, $0 \le \alpha \le 1$ is the *reflection coefficient* (RC) at the BDs, and $z_1(k;n)$ and $z_2(k;n)$ denote the additive Gaussian noise. It should be noted integrated circuits in BDs do not include any active radio frequency components such as oscillators, analog-to-digital converters, and power amplifiers. Therefore, the noise at the BDs is very low and usually assumed to be neglected as in [11].

The desired signals at the UAV and DC are $s_m(k;n)$ and $s_m(k;n-\tau)$, respectively. Meanwhile, τ is large enough so that $s_m(k;n)$ and $s_m(k;n-\tau)$ are independent. Thus, the *signal-to-interference-plus-noise ratio* (SINR) of the first and second hop is given by

$$\text{SINR}_{m,k}^{(1)} = \frac{h_m[k]\alpha P_k}{\delta^2 + \zeta P_k}, \quad (3)$$

$$\text{SINR}_{m,k}^{(2)} = \frac{g[k]P_k}{\delta^2}, \quad (4)$$

respectively. It should be noted that the interference from the BD to the DC is ignored in (4), due to the long distance in between. Then, the transmit rate from BD m to the DC in time slot k is

$$R_{m,k} = \min\left(R_{m,k}^{(1)}, R_{m,k}^{(2)}\right), \quad (5)$$

where $R_{m,k}^{(1)} = \log\left(1 + \text{SINR}_{m,k}^{(1)}\right)$ and $R_{m,k}^{(2)} = \log\left(1 + \text{SINR}_{m,k}^{(2)}\right)$.

2.2. Problem Formulation. We aim to maximize the minimum average rate among all BDs while avoiding severe interference to the CU via joint time scheduling, transmit power control, and UAV trajectory design over all time slots. Define $B = \{\beta_{m,k}, \forall m,k\}$, $Q = \{q_k, \forall k\}$, and $P = \{P_k, \forall k\}$. Then, the optimization problem can be mathematically formulated as

$$\max_{\{B,Q,P\}} G(B,Q)\Delta = \min_m \frac{1}{K}\sum_{k=1}^{K} \beta_{m,k}R_{m,k}, \quad (6)$$

$$\text{s.t.} \sum_{m=1}^{M} \beta_{m,k} \le 1, \forall k \in \{1,\cdots,K\}, \quad (7a)$$

$$\|q_{k+1} - q_k\| \le \frac{v_{\max}T}{K}, \forall k \in \{0,\cdots,K-1\}, \quad (7b)$$

$$q_0 = q_K, \quad (7c)$$

$$g_0[k]P_k \le \lambda, \forall k \in \{1,\cdots,K\}, \quad (7d)$$

$$P_k \le P_{\max}, \forall k \in \{1,\cdots,K\}, \quad (7e)$$

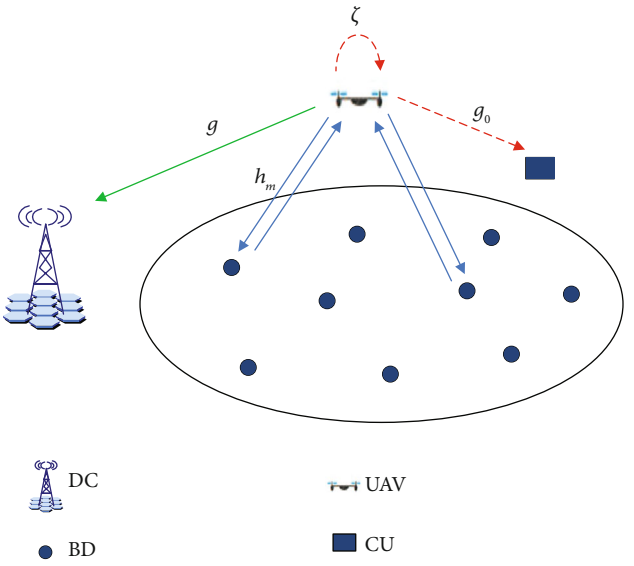

Figure 1: System model for a UAV-assisted backscatter network.

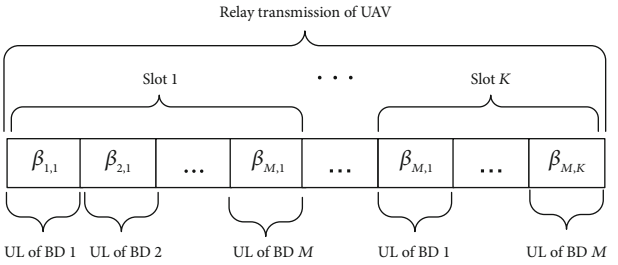

Figure 2: Frame structure for a UAV-assisted backscatter network.

where $v_{\max}$ is the maximum speed of the UAV, q_0 is the initial location of the UAV, λ is the interference threshold at the CU, and $P_{\max}$ is the maximum transmit power of the UAV. Constraint (7a) is originated from the fact that the overall length of assigned time should not exceed the total time slot length. Constraint (7b) is the flight speed constraint, and constraint (7c) implies that the UAV will return to the initial point at the end of the whole time period. Constraints (7d) and (7e) define the feasible transmit power of the UAV at any time slot. It should be noted that the interference from BDs to the CU is ignored in (7d), because the power of backscatter signals are much smaller than the original incident signal in general.

The above problem is challenging to solve directly, because the objective function in (6) is nonconvex with respect to B, Q, and P. In addition, B, Q, and P are coupled in the constraints. Therefore, instead of solving it directly, we use the BCD method to deal with it in the following section.

3. Proposed Algorithm

To solve problem (4), we propose the following iterative algorithm, which applies the BCD to partitioning the variables

into two blocks, i.e., the time scheduling and power control variable $\{B, P\}$ and the UAV trajectory variable Q

$$\underbrace{Q^{(0)}}_{\text{Initialization}} \to \cdots \to \underbrace{\left\{B^{(n-1)}, P^{(n-1)}\right\} \to Q^{(n-1)}}_{(n-1)-\text{th iteration}} \to \underbrace{\left\{B^{(n)}, P^{(n)}\right\} \to Q^{(n)}}_{n-\text{th iteration}} \to \cdots \to \underbrace{\{B^*, P^*\} \to Q^*}_{\text{optimal solution}}. \tag{8}$$

Specially, the algorithm starts by finding an initial UAV trajectory $Q^{(0)}$. At each iteration n, it first derives $\{B^{(n)}, P^{(n)}\}$ for given $Q^{(n-1)}$ from the last iteration and then finds $Q^{(n)}$ for the fixed $\{B^{(n)}, P^{(n)}\}$. The process is repeated until no further improvement is obtained. In the following, we first present the solution for $\{B, P\}$ and Q, respectively. Then, we propose a novel method to find the initial trajectory of the UAV. Finally, we give the whole procedure of the proposed algorithm and prove its convergence.

3.1. Optimal Time Scheduling and Power Control. Given the UAV trajectory $Q^{(n-1)}$, the optimal time scheduling and power control can be obtained by solving the following problem:

$$\max_{\{B,P,\eta\}} \eta, \tag{9}$$

$$\text{s.t.} \frac{1}{K}\sum_{k=1}^{K} \beta_{m,k} R_{m,k} \geq \eta, \forall m, \tag{10a}$$

$$\sum_{m=1}^{M} \beta_{m,k} \leq 1, \forall m, \tag{10b}$$

$$g_0[k] P_k \leq \lambda, \forall k \in \{1, \cdots, K\}, \tag{10c}$$

$$P_k \leq P_{\max}, \forall k \in \{1, \cdots, K\}, \tag{10d}$$

where η is the auxiliary variable. This problem is convex with B and P, and a two-step method is propose to deal with the transmit power control and time scheduling sequentially.

Since the value of $g_0[k]$ is known when $Q^{(n-1)}$ is given, the optimal transmit power to the above problem is

$$P_k = \max\left(P_{\max}, \frac{\lambda}{g_0[k]}\right). \tag{11}$$

Then, with P_k given in (11), $R_{m,k}$ is known, and problem (9) becomes a standard linear programming problem in B. Therefore, we can adopt the interior-point method to deal the time scheduling in polynomial time [22].

3.2. UAV Trajectory Design. For the given transmit power and time scheduling $\{B^{(n)}, P^{(n)}\}$, problem (4) is simplified as the UAV trajectory design problem as follows

$$\max_{\{Q,\eta\}} \eta, \tag{12}$$

$$\text{s.t.} \frac{1}{K}\sum_{k=1}^{K} \beta_{m,k} \bar{R}_{m,k} \geq \eta, \forall m, \tag{13a}$$

$$\bar{R}_{m,k} \leq R_{m,k}^{(1)}, \forall m, \tag{13b}$$

$$\bar{R}_{m,k} \leq R_{m,k}^{(2)}, \forall m, \tag{13c}$$

$$\|q_{k+1} - q_k\| \leq \frac{v_{\max} T}{K}, \forall k \in \{0, \cdots, K-1\}, \tag{13d}$$

$$q_0 = q_K, \tag{13e}$$

$$g_0[k] P_k \leq \lambda, \forall k \in \{1, \cdots, K\}, \tag{13f}$$

where both η and $\bar{R}_{m,k}$ are the auxiliary variables.

It is obvious that both $R_{m,k}^{(1)}$ and $R_{m,k}^{(2)}$ are nonconcave with respect to Q. To solve the problem, we first need to reshape $R_{m,k}^{(1)}$ and $R_{m,k}^{(2)}$ into more trackable forms.

Set $C_{m,k}^{(1)}(q_k) = (\tau P + \delta^2)[(H - H_m)^2 + \|q_k - l_m\|^2]^2$, $C_{m,k}^{(2)}(q_k) = \delta^2(H^2 + \|q_k\|^2)$, $A_1 = \gamma_1 \alpha P$, and $A_2 = \gamma_2 P$. Then, we have

$$R_{m,k}^{(1)} = \log\left(1 + \frac{A_1}{C_{m,k}^{(1)}(q_k)}\right), \tag{14}$$

$$R_{m,k}^{(2)} = \log\left(1 + \frac{A_2}{C_{m,k}^{(2)}(q_k)}\right). \tag{15}$$

Apparently, both A_1 and A_2 are constant, while $C_{m,k}^{(1)}$ and $C_{m,k}^{(2)}$ are convex with respect to q_k. Therefore, the above problem is a concave-convex FP problem, which can be efficiently solved by the FP method proposed in [20].

The main idea of the proposed FP method is to transform problem (12) into a sequence of convex optimization problems by reshaping the fractional terms within $R_{m,k}^{(1)}$ and $R_{m,k}^{(2)}$ into quadratic structures. Denote $\bar{Q}^{(l)} = \{\bar{q}^{(l)}, \forall k\}$ as the fixed

point at the l-th iteration in the FP method. Then, problem (12) can be solved by the following sequence programming

$$\left\{\bar{Q}^{(l+1)}, \eta^*, \bar{R}^*_{m,k}\right\} = \underset{\left\{Q,\eta,\bar{R}_{m,k}\right\}}{\operatorname{argmax}} \eta, \tag{16}$$

$$\text{s.t.} \frac{1}{K}\sum_{k=1}^{K} \beta_{m,k}\bar{R}_{m,k} \geq \eta, \forall m, \tag{17a}$$

$$\bar{R}_{m,k} \leq \widehat{R}^{(1)}_{m,k}, \forall m, \tag{17b}$$

$$\bar{R}_{m,k} \leq \widehat{R}^{(2)}_{m,k}, \forall m, \tag{17c}$$

$$\|q_{k+1} - q_k\| \leq \frac{v_{\max}T}{K}, \forall k \in \{0, \cdots, K-1\}, \tag{17d}$$

$$q_0 = q_K, \tag{17e}$$

where $\widehat{R}^{(1)}_{m,k}$ and $\widehat{R}^{(2)}_{m,k}$ are given by

$$\widehat{R}^{(1)}_{m,k} = \log\left[1 + 2y^{(l)}_{m,k}\sqrt{A_1} - \left(y^{(l)}_{m,k}\right)^2 C^{(1)}_{m,k}(q_k)\right], \tag{18}$$

$$\widehat{R}^{(2)}_{m,k} = \log\left[1 + 2z^{(l)}_{m,k}\sqrt{A_2} - \left(z^{(l)}_{m,k}\right)^2 C^{(2)}_{m,k}(q_k)\right], \tag{19}$$

respectively, $y^{(l)}_{m,k} = \sqrt{A_1}/C^{(1)}_{m,k}(\bar{q}^{(l)}_k)$, and $z^{(l)}_{m,k} = \sqrt{A_2}/C^{(2)}_{m,k}(\bar{q}^{(l)}_k)$.

In general, the FP method can start with any feasible Q. The BCD is adopted as an outer loop for the FP method in this paper; however, we set $\bar{Q}^{(0)} = Q^{(n-1)}$ to guarantee the convergence of the proposed algorithm. It is apparent that problem (16) is a standard convex optimization problem at each iteration l. Thus, we adopt CVX to solve it.

The whole procedure of the proposed FP method is summarized as Algorithm 1, and its effectiveness is shown in the following theorem, which is proved in Appendix A.

Theorem 1. *With sequential programming given in (16), Algorithm 1 generates a sequence $\bar{Q}^{(l)}$ rendering a increasing value of η, which finally converges to a local optimum η^*.*

3.3. Trajectory Initialization Method. In this subsection, we use the simple circular trajectory to initialize the UAV trajectory $Q^{(0)}$. That is, the initial trajectory of the UAV is set to be a circular with a constant speed of v, where $0 \leq v \leq v_{\max}$.

Define w_m as the optimal relay location for BD m. Then, w_m can be obtained from the following theorem, which is proved in Appendix B.

Theorem 2. *Define $D = \|l_m\|$. Then, w_m is given by*

$$w_m = \begin{cases} l_m, & \text{if } F(D) \geq 0, \\ [0,0]^T, & \text{if } F(D) \leq 0, \\ \mu l_m, & \text{otherwise}, \end{cases} \tag{20}$$

where

$$F(x) = \gamma_2\left(\tau P_{\max} + \delta^2\right)\left[(H - H_m)^2 + (D - x)^2\right]^2 - \gamma_1\alpha\delta^2\left(H^2 + x^2\right), \tag{21}$$

and $\mu = F^{-1}(0)/D$. $F^{-1}(x)$ is the inverse function of $F(x)$.

Intuitively, the UAV's trajectory should cover as many w_m as possible. Therefore, the center of the circular trajectory is the geometric center of all w_m, i.e., $c = \sum_{m=1}^{M} w_m/M$, and the radius of the circular trajectory should satisfy

$$r = \min\left[\max_m \|w_m - c\|, \frac{v_{\max}T}{2\pi}\right], \tag{22}$$

where the first term is the minimum radius to cover all w_m, and the second term is the maximum radius due to the UAV speed constraint. Based on c and r, the initial trajectory of the UAV is given by

$$q^{(0)}_k = c + [r\cos(\theta_k), r\sin(\theta_k)]^T, \forall k, \tag{23}$$

where $\theta_k = (2\pi(k-1))/(K-1)$.

3.4. Overall Algorithm and Convergence. We summarize the proposed iterative algorithm as Algorithm 2, which handles joint time scheduling, transmit power control, and UAV trajectory design based on the BCD and FP methods. Specially, the algorithm starts by designing the initial UAV trajectory $Q^{(0)}$ as in Section 3.3. Given a fixed $Q^{(n-1)}$ in the $(n-1)$-th iteration, $P^{(n)}$ is obtained from (11), and $B^{(n)}$ is determined by using the interior-point method given in Section 3.1. Then, for a fixed $\{B^{(n)}, P^{(n)}\}$, $Q^{(n)}$ is obtained by applying the FP method in Algorithm 1. The process repeats until the convergence condition is satisfied. The convergence of the algorithm is analyzed in the following theorem, which is proved in Appendix C.

Theorem 3. *For problem (6), the proposed iterative algorithm in Algorithm 2 generates a sequence of $\{B^{(n)}, P^{(n)}, Q^{(n)}\}$ rendering $G(B^{(n)}, P^{(n)}, Q^{(n)}) \geq G(B^{(n-1)}, P^{(n-1)}, Q^{(n-1)})$, which finally converges to a local optimal solution $\{B^*, P^*, Q^*\}$.*

Although the convergence speed of the FP and BCD methods cannot be analyzed theoretically [20, 23], both methods converge typically in a few iterations for a moderate number of BDs as will be numerically shown in Section 4. Meanwhile, the trajectory design problem in each iteration of the FP algorithm and the time scheduling and transmit power control problem in each iteration of the BCD method are all convex optimization problems, which can be solved in polynomial time. Therefore, the time complexity of the proposed iterative method is polynomial, and it can be practically implemented with fast convergence for a UAV-assisted cognitive AmBC system with a moderate number of BDs.

Initialize:
  $l = 0$, $\bar{\mathrm{Q}}^{(0)} = \mathrm{Q}^{(n-1)}$, tolerance $\sigma > 0$;
Repeat:
  Update $y_{m,k}^{(l)} = \sqrt{A_1}/C_{m,k}^{(1)}(\bar{q}_k^{(l)})$ and $z_{m,k}^{(l)} = \sqrt{A_2}/C_{m,k}^{(2)}(\bar{q}_k^{(l)})$;
  Reshape $\widehat{R}_{m,k}^{(1)}$ and $\widehat{R}_{m,k}^{(2)}$ by (18) and (19), respectively;
  Solve the reformulated convex problem in (16) by CVX;
  $l = l + 1$;
Until: $\|\bar{\mathrm{Q}}^{(l)} - \bar{\mathrm{Q}}^{(l-1)}\| \le \sigma$;
  Set $\mathrm{Q}^{(n)} = \bar{\mathrm{Q}}^{(l)}$.

Algorithm 1: FP algorithm. FP method for UAV trajectory design.

Initialize:
  Set $n = 0$, tolerance $\sigma > 0$;
  Set $\mathrm{Q}^{(0)}$ according to Section III-C;
Repeat:
  Set $n = n + 1$;
  For fixed $\mathrm{Q}^{(n-1)}$, $\mathrm{P}^{(n)}$ is obtained from (11), and $\mathrm{B}^{(n)}$ is obtained by the interior-point method;
  For fixed $\{\mathrm{B}^{(n)}, \mathrm{P}^{(n)}\}$, $\mathrm{Q}^{(n)}$ is found by the FP method in Algorithm 1;
Until: $|\mathrm{G}(\mathrm{B}^{(n)}, \mathrm{P}^{(n)}, \mathrm{Q}^{(n)}) - \mathrm{G}(\mathrm{B}^{(n-1)}, \mathrm{P}^{(n-1)}, \mathrm{Q}^{(n-1)})| \le \sigma$;
  Set $\{\mathrm{B}^*, \mathrm{P}^*, \mathrm{Q}^*\} = \{\mathrm{B}^{(n)}, \mathrm{P}^{(n)}, \mathrm{Q}^{(n)}\}$;
Return: $\{\mathrm{B}^*, \mathrm{P}^*, \mathrm{Q}^*\}$.

Algorithm 2: The iterative algorithm to problem (6). The procedure of proposed iterative algorithm.

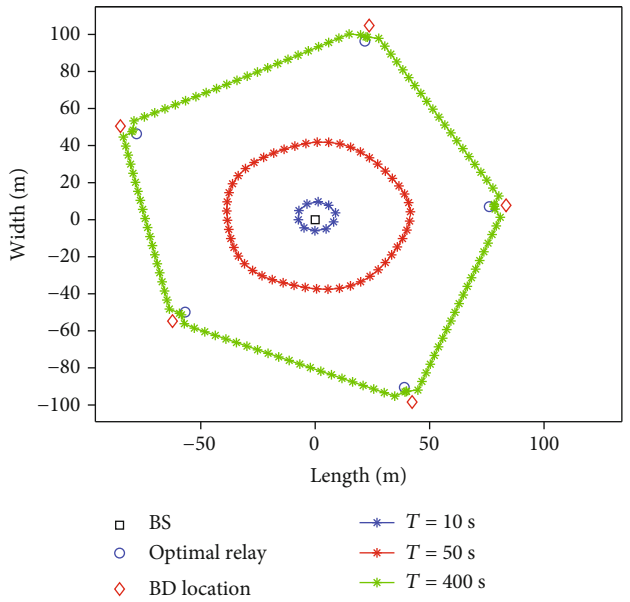

Figure 3: The UAV trajectory of the proposed algorithm for different time periods.

4. Simulation Results

In this section, we provide simulation results to verify the effectiveness of the proposed algorithm in Algorithm 2. We consider a UAV-assisted cognitive backscatter network as shown in Figure 3, where the DC is located in the cell center, and 5 BDs are randomly distributed within the area with the radius of 200 m. The UAV flies at a fixed height of 10 m, and its maximum flight speed is 20 m/s. In the simulation, we set the transmit power of the UAV and the power spectrum density of the noise to be 30 dBm and −139 dBm/Hz, respectively. In addition, other parameters are set as $\gamma_1 = 0.001$, $\gamma_2 = 0.01$, $\tau = -110$ dB, and $\alpha = 0.5$.

Figure 3 illustrates the UAV trajectory of the proposed algorithm for different time periods T. From the figure, we can observe that the UAV adaptably enlarge and adjust its trajectory to approach the optimal relay locations of BDs when T changes. Specially, when T is sufficiently large, i.e., $T = 400$ s, the UAV is able to visit all these optimal locations one by one. In this case, the trajectory of the UAV becomes a close loop with segments connecting all these points, and the UAV tends to spend more time near these points (flies much slower) to obtain better communication links.

Figure 4 illustrates the performance of the proposed algorithm for different time periods T. For comparison, we also investigate the *circular trajectory* (CT) and *static location* (SL) algorithms [21] in the simulation. Specially, the CT algorithm utilizes the initial circular trajectory, while the SL one requires that the UAV hovers statically over the geometric center of the optimal relay locations. It should be noted that both algorithms adopt the linear programming algorithm proposed in Section 3.1 to solve the time scheduling problem. From the figure, the average max-min rate of the SL method is independent with T since the links of the first and second

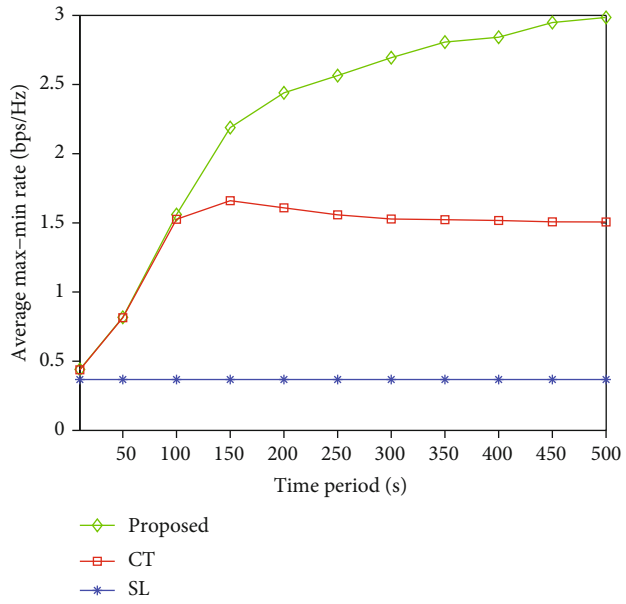

Figure 4: The average max-min rate of the proposed algorithm for different time periods.

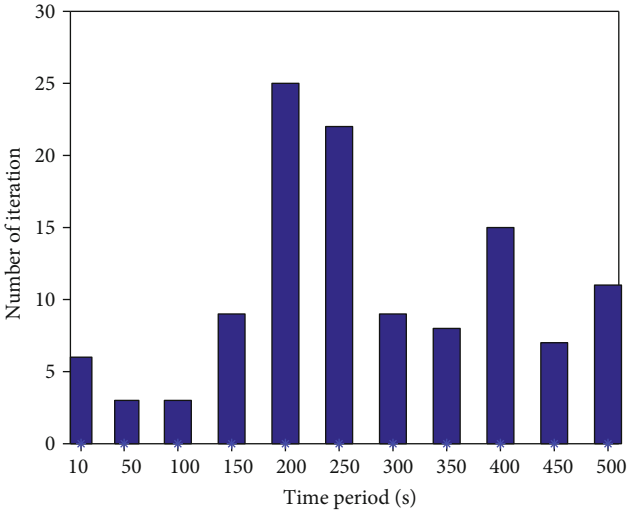

Figure 5: The complexity of the proposed algorithm for different time periods.

hops are all time invariant for a static UAV. In comparison, the average max-min rate of the proposed algorithm increases with T and becomes saturated when T is sufficient large. This is expected because the UAV is able to adjust its trajectory and flight speed to spend more time near the locations rendering better communication channels. Thus, the average max-min rate increases with T. For the CT method, however, the UAV cannot change its flight speed. Thus, when T exceeds a certain amount, i.e., $T = 150$ s, increasing T may increase the time spent on those undesirable area. As a result, the average max-min rate of the CT algorithm slightly decreases when T is larger than 150 s.

Figure 5 illustrates the complexity of the proposed algorithm for different T. It can be easily observe from the figure that the proposed algorithm at most takes 25 iterations to converge, which demonstrates the effectiveness of the proposed algorithm. Meanwhile, it cannot find any law for the iteration times of the FP algorithm for different T. This also consistent with the fact that the complexity of the FP is difficult to derive theoretically [20].

5. Conclusions

In this paper, we have studied joint trajectory design and spectrum management for a UAV-assisted cognitive backscatter network to optimize the average max-min uplink rate of BDs. To achieve this objective, we have proposed an iterative method utilizing BCD to partition the variables into two blocks. For the time scheduling and power control problem, the interior-point method has been proposed to solve it, while for the trajectory design one, the FP method has been adopted. Both the convergence and complexity of the proposed algorithm have been demonstrated by simulation results.

Appendix

A. Proof for Theorem 1

Since the logarithm function is concave and nondecreasing and $C_{m,k}^{(1)}(q_k)$ and $C_{m,k}^{(2)}(q_k)$ are convex, the sequence updates in (14) and (15) make $\widehat{R}_{m,k}^{(1)}$ and $\widehat{R}_{m,k}^{(2)}$ a nondecreasing manner according to Theorem 3 in [20]. Meanwhile, the optimal η^* is obtained, when the equalities in constraints (17a)–(17c) are achieved. As a result, η increases with the iteration number l. Since the feasible region defined by constraints (17d) and (17e) is finite, η must converge to a local optimal value of η^*, which completes the proof.

B. Proof for Theorem 2

Since the channel model only considers the distance-based path-loss, the optimal relay location must be on the straight line between the DC and BD m. Denote $x \in [0, D]$ as the distance between the DC and the UAV. Obviously, $R_{m,k}^{(1)}$ is increasing in x, while $R_{m,k}^{(2)}$ is decreasing. Therefore, if $F(D) \geq 0$, it means $R_{m,k}^{(2)} \geq R_{m,k}^{(1)}$ even when $x = D$. In this case, $w_m = l_m$. Similarly, if $F(0) \leq 0$, $R_{m,k}^{(2)} \leq R_{m,k}^{(1)}$ even when $x = 0$. Then, $w_m = [0, 0]^T$. If $F(0) > 0$ and $F(D) < 0$, there exists a unique $x \in [0, D]$ making $R_{m,k}^{(2)} = R_{m,k}^{(1)}$, i.e., $F(x) = 0$. In this case, $w_m = (F^{-1}(0)/D)l_m$, which completes the proof.

C. Proof for Theorem 3

Theorem 1 has shown that the FP method generates a sequence of convex optimization problems converging to a stationary point with nondecreasing manner after each iteration. Therefore, we can obtain $G(B^{(n)}, P^{(n)}, Q^{(n+1)}) \geq G(B^{(n)}, P^{(n)}, Q^{(n)})$. Meanwhile, the optimal $B^{(n)}$ and $P^{(n)}$ to problem (6) can be obtained via interior-point method and (11),

respectively. Therefore, $G(B^{(n+1)}, P^{(n+1)}, Q^{(n+1)}) \geq G(B^{(n)}, P^{(n)}, Q^{(n)})$ is also obtained. Since the solution region is compact, the iterative method proposed in Algorithm 2 can finally converge to a local optimal point $\{B^*, P^*, Q^*\}$, and this completes the proof.

Data Availability

As this work is supported by the following funding, the data is not allowed to publish online by the funder.

Conflicts of Interest

The authors declare that they have no conflicts of interest.

Acknowledgments

The work is supported in part by the National Nature Science Foundation of China under Grant No. 62001094, the Guangdong Basic and Applied Basic Research Foundation under Grant No. 2019A1515111162 and 2019A1515110900, and the Fundamental Research Funds for the Central Universities under Grant ZYGX2016KYQD143.

References

[1] J. Gubbi, R. Buyya, S. Marusic, and M. Palaniswami, "Internet of Things (IoT): a vision, architectural elements, and future directions," *Future generation computer systems*, vol. 29, no. 7, pp. 1645–1660, 2013.

[2] X. Liu and X. Zhang, "NOMA-based resource allocation for cluster-based cognitive industrial internet of things," *IEEE transactions on industrial informatics*, vol. 16, no. 8, pp. 5379–5388, 2020.

[3] A. A. Khan, M. H. Rehmani, and A. Rachedi, "Cognitive-radio-based internet of things: applications, architectures, spectrum related functionalities, and future research directions," *IEEE Wireless Communications*, vol. 24, no. 3, pp. 17–25, 2017.

[4] L. Zhang, Y. Liang, and M. Xiao, "Spectrum sharing for internet of things: a survey," *IEEE Wireless Communications*, vol. 26, no. 3, pp. 132–139, 2019.

[5] X. Liu, X. B. Zhai, W. Lu, and C. Wu, "QoS-guarantee resource allocation for multibeam satellite industrial internet of things with NOMA," *IEEE Transactions on Industrial Informatics*, vol. 17, no. 3, pp. 2052–2061, 2021.

[6] X. Liu and X. Zhang, "Rate and energy efficiency improvements for 5g-based iot with simultaneous transfer," *IEEE Internet of Things Journal*, vol. 6, no. 4, pp. 5971–5980, 2019.

[7] B. Kellogg, A. Parks, S. Gollakota, J. R. Smith, and D. Wetherall, "Wi-Fi backscatter: Internet connectivity for RF-powered devices," in *Proceedings of the 2014 ACM Conference on SIGCOMM*, vol. 44no. 4, pp. 607–618, 2014.

[8] A. N. Parks, A. Liu, S. Gollakota, and J. R. Smith, "Turbocharging ambient backscatter communication," *ACM SIGCOMM Computer Communication Review*, vol. 44, no. 4, pp. 619–630, 2015.

[9] V. Liu, A. Parks, V. Talla, S. Gollakota, D. Wetherall, and J. R. Smith, "Ambient backscatter," *ACM SIGCOMM computer communication review*, vol. 43, no. 4, pp. 39–50, 2013.

[10] N. V. Huynh, D. T. Hoang, X. Lu, D. Niyato, P. Wang, and D. I. Kim, "Ambient backscatter communications: a contemporary survey," *IEEE Communications Surveys & Tutorials*, vol. 20, no. 4, pp. 2889–2922, 2018.

[11] S. Xiao, H. Guo, and Y. Liang, "Resource allocation for full-duplex-enabled cognitive backscatter networks," *IEEE Transactions on Wireless Communications*, vol. 18, no. 6, pp. 3222–3235, 2019.

[12] H. Guo, Q. Zhang, S. Xiao, and Y. Liang, "Exploiting multiple antennas for cognitive ambient backscatter communication," *IEEE Internet of Things Journal*, vol. 6, no. 1, pp. 765–775, 2019.

[13] W. Lu, X. Xu, G. Huang et al., "Energy-efficient scheduling of distributed flow shop with heterogeneous factories: a real-world case from automobile industry in China," *IEEE Transactions on Industrial Informatics*, p. 1, 2020.

[14] Y. Zeng, R. Zhang, and T. J. Lim, "Wireless communications with unmanned aerial vehicles: opportunities and challenges," *IEEE Communications Magazine*, vol. 54, no. 5, pp. 36–42, 2016.

[15] Q. Wu, L. Liu, and R. Zhang, "Fundamental trade-offs in communication and trajectory design for UAV-enabled wireless network," *IEEE Wireless Communications*, vol. 26, no. 1, pp. 36–44, 2019.

[16] Y. Zeng and R. Zhang, "Energy-efficient UAV communication with trajectory optimization," *IEEE Transactions on Wireless Communications*, vol. 16, no. 6, pp. 3747–3760, 2017.

[17] S. Zhang, H. Zhang, Q. He, K. Bian, and L. Song, "Joint trajectory and power optimization for UAV relay networks," *IEEE Communications Letters*, vol. 22, no. 1, pp. 161–164, 2018.

[18] Y. Ma, N. Selby, and F. Adib, "Drone relays for battery-free networks," in *Proceedings of the Conference of the ACM Special Interest Group on Data Communication*, pp. 335–347, 2017.

[19] P. Tseng, "Convergence of a block coordinate descent method for nondifferentiable minimization," *Journal of optimization theory and applications*, vol. 109, no. 3, pp. 475–494, 2001.

[20] K. Shen and W. Yu, "Fractional programming for communication systems—part I: power control and beamforming," *IEEE Transactions on Signal Processing*, vol. 66, no. 10, pp. 2616–2630, 2018.

[21] Q. Wu, Y. Zeng, and R. Zhang, "Joint trajectory and communication design for multi-UAV enabled wireless networks," *IEEE Transactions on Wireless Communications*, vol. 17, no. 3, pp. 2109–2121, 2018.

[22] D. Bertsimas and J. N. Tsitsiklis, *Introduction to Linear Optimization*, vol. 6, Athena Scientific, Belmont, MA, 1997.

[23] D. T. Ngo, S. Khakurel, and T. Le-Ngoc, "Joint subchannel assignment and power allocation for OFDMA femtocell networks," *IEEE Transactions on Wireless Communications*, vol. 13, no. 1, pp. 342–355, 2014.